



Agenzia Nazionale per le Nuove Tecnologie,
l'Energia e lo Sviluppo Economico Sostenibile



Ministero dello Sviluppo Economico

RICERCA DI SISTEMA ELETTRICO

Analysis of the impact of the heavy reflector of a typical large size
GEN III+ reactor design on the ex-core detector signals with Monte
Carlo techniques (Employing MCNP-5)

K.W. Burn

ANALYSIS OF THE IMPACT OF THE HEAVY REFLECTOR OF A TYPICAL LARGE SIZE GEN III+ REACTOR DESIGN ON THE EX-CORE DETECTOR SIGNALS WITH MONTE CARLO TECHNIQUES (EMPLOYING MCNP-5)

K.W. Burn (ENEA)

Novembre 2011

Report Ricerca di Sistema Elettrico

Accordo di Programma Ministero dello Sviluppo Economico – ENEA

Area: Governo, gestione e sviluppo del sistema elettrico nazionale

Progetto: Fissione nucleare: metodi di analisi e verifica di progetti nucleari di generazione evolutiva ad acqua pressurizzata

Responsabile Progetto: Massimo Sepielli, ENEA

Titolo

Analysis of the Impact of the Heavy Reflector of a Typical Large Size GEN III+ Reactor Design on the Ex-Core Detector Signals with Monte Carlo Techniques (Employing MCNP-5)

Descrittori

Tipologia del documento:

Collocazione contrattuale: ACCORDO DI PROGRAMMA Ministero dello Sviluppo Economico – ENEA sulla Ricerca di Sistema Elettrico PIANO ANNUALE DI REALIZZAZIONE 2010 Progetto 1.3.2.a: Fissione nucleare: Metodi di analisi e verifica di progetti nucleari di generazione evolutiva ad acqua pressurizzata.

Argomenti trattati:Reattori nucleari ad acqua, Neutronica, Schermaggio delle radiazioni, Metodi Montecarlo

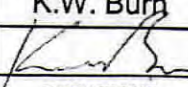
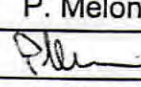
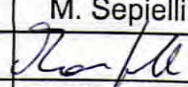
Sommario

Some analysis is made of the impact of the heavy steel reflector of a typical large size GEN III+ reactor design on some neutronic safety features during start-up. The analysis is made with the Monte Carlo code MCNP5 (with in-house modifications)."

Note

Copia n.


In carico a:

2			NOME			
			FIRMA			
1			NOME			
			FIRMA			
0	EMISSIONE	18/11/2011	NOME	K.W. Burn	P. Meloni	M. Sepielli
			FIRMA			
REV.	DESCRIZIONE	DATA	REDAZIONE	CONVALIDA	APPROVAZIONE	

Indice

1. Introduction
2. Fundamental Fission Mode
 - 2.1 Nuclear Data
 - 2.2 Geometry
 - 2.3 Boron Concentration in the Water
 - 2.4 Calculation of the Neutron Source
 - 2.5 Neutron Source Coupling
 - 2.6 Ex-Core Transport
3. ^{252}Cf Start-Up Sources
 - 3.1 Geometry
 - 3.2 ^{252}Cf Sources – to – Fundamental Mode
 - 3.3 Ex-Core Transport
4. Fast Neutron Flux
5. Summary
6. Next Steps


Appendix: the DSA

 Ricerca Sistema Elettrico	Sigla di identificazione PAR2010-ENEA-LD2-010	Rev. 0	Distrib. L	Pag. 3	di 15
--	---	------------------	----------------------	------------------	-----------------

1. Introduction

This work has been performed within the framework of an agreement between ENEA and IRSN (Institut de Radioprotection et de Sûreté Nucléaire). The particular area of the activity deals with safety issues concerning the thick steel reflector of a typical large size GEN III+ reactor design and in particular the differences caused by this reflector compared with current PWR designs.

As much of the data employed was confidential, this report is by necessity in a condensed form. A detailed confidential document is also being issued.

 Ricerca Sistema Elettrico	Sigla di identificazione	Rev.	Distrib.	Pag.	di
	PAR2010-ENEA-LD2-010	0	L	4	15

2. Fundamental Fission Mode

2.1 Nuclear Data

As far as the employed neutron cross-section data were concerned, the defined model was Hot Zero Power (303.3°C) (IRSN DSR/ST3C/2011-29). A mixture of public and in-house (see acknowledgement) data were employed. The elastic scattering cross-section in the thermal range was adjusted to 303.3°C with the free gas thermal treatment model for cross-sections of all materials within the PV including the vessel itself. (Also with the same model the velocity of the target nucleus was adjusted to 303.3°C.) Instead for cross-sections of all materials outside the PV, a temperature of 20°C was employed for the thermal treatment with the free gas model. Then below typically 4 eV, $S(\alpha,\beta)$ data were employed, where available.

2.2 Geometry


The geometrical model for the fundamental fission mode calculations employed a pin-by-pin description. The supplied geometry data [IRSN DSR/ST3C/2011-29 and following exchange of e-mails (see acknowledgement)] allowed a 1/8 azimuthal segment with reflection surfaces to model the whole core. The plena regions and top and bottom plate data were not supplied and typical PWR configurations were employed. Also the situation of the geometry below the core including the pressure vessel (PV) curvature was not supplied and, again, typical PWR configurations were employed.

For the generation of the fundamental mode fission source, the homogenised heavy reflector model was used (IRSN DSR/ST3C/2011-29). To model a current generation PWR, this reflector was then made water. Finally a 1 inch thick baffle was added to this water reflector model to verify some of the in-core results. Thus for the eigenvalue (core) calculations, three models were employed: thick steel reflector; all water reflector; all water reflector with steel baffle.

2.3 Boron Concentration in the Water

Boric acid is dissolved in the primary reactor coolant water. Its concentration is varied so as to maintain full power as the fuel is burnt. The concentration of the boron in the water to obtain criticality with fresh fuel was not *a priori* known (by us) and in any case would depend on the particular geometrical model that we employed.

The search for the appropriate concentration of boron was made at two states: criticality and $k_{\text{eff}} = 0.95$. (Note that the variation between the shut-down state of $k_{\text{eff}} = 0.95$ and criticality would in reality also be achieved through control rod movement. Instead here for ease of calculation it was accomplished through the boron concentration only leaving the control rods in the same position as at criticality.) This was done for the homogeneous heavy steel reflector. Values of the boron concentration were found to achieve the above two criticality levels. The water reflector changes slightly the criticality level but the comparisons between the reflectors were made at these boron concentrations. (Note however a compensatory factor was applied to the results with the water reflector in some cases.) As expected, the curve of k_{eff} against boron concentration in the water shows a slight convex shape due to partial saturation.

 Ricerca Sistema Elettrico	Sigla di identificazione	Rev.	Distrib.	Pag.	di
	PAR2010-ENEA-LD2-010	0	L	5	15

2.4 Calculation of the Neutron Source

To generate the fixed fission source which is then employed to transport the neutrons out of the core and through the reflector, downcomer and PV, the classic “bootstrapping” approach was adopted. Thus an eigenvalue calculation was first executed to write the fundamental fission mode source. There are a number of issues around such a calculation on a full size (albeit 1/8 segment) PWR core, among which are the convergence of the fission source to the fundamental mode and the correlations between fission cycles.

In a standard fashion, starting with a point source at the centre of the geometry and with a small number (of the order of a few hundred) of fission neutrons per cycle, the number of fission neutrons per cycle was increased in a number of steps to some tens of thousands, with at each step a few hundred cycles being run. Finally 100 cycles of 50000 neutrons per cycle were run, followed by 10 cycles each of 250000 neutrons. At this point it was assumed that the source was converged. Shannon entropy and other standard MCNP diagnostics were used to verify the state of the source convergence. It should be mentioned that separate fundamental modes were generated for the heavy steel reflector, for the water reflector and for the water reflector + baffle.

[Although it was believed that source convergence was achieved, the procedure was not fully documented. Poor source convergence has been considered as a reason for power profiles in the core that seem anomalous – see following paragraphs. However current independent calculations (concerning the evaluation of the secondary start-up source strengths) on a full – not 1/8 – core model with an extremely long and documented source convergence procedure seem to confirm the results. Finally it should be mentioned that these issues hardly affect the final results of this work, namely the ex-core detector responses.]


Some comparisons between the in-house neutron data and the public data (albeit Doppler broadened to a different temperature) showed no difference in the integral results for the fission source in the five assembly types (see IRSN DSR/ST3C/2011-29). There is however some difference between the three reflector models.

Some differential profiles for the pin-by-pin power (i.e. fission source) were also generated and compared for the different reflectors. There are three points to note:

- 1) The outer pin of the outer assembly showed a relatively large power ratio [water/steel reflector or (water+baffle)/steel reflector] for the different reflectors.
- 2) From the central pin of the outer assembly, inwards until the assemblies in the 3rd-to-outer ring the above ratio flips to below 1. It then goes above 1 for the inner assemblies.
- 3) The above ratio showed surprisingly large values near the core centre.

The above items 1 and 2 reflect the trade-off between a greater reflection of epithermal neutrons by the steel compared with the water and a greater thermal neutron absorption in the steel and were as expected. Instead the above item 3 looked unexpectedly high. Comparisons between the in-house and public neutron data seem to indicate that the problem does not lie in the in-house generation of the neutron data.

Some effort was made to try to verify the above seemingly anomalous item 3 by comparing with other independently-generated results (see acknowledgement). Assembly-by-assembly power profiles were provided for three other configurations. Unfortunately these configurations are quite different both from each other and from that considered here. [However just for the configuration considered here, the profile with the water reflector is substantially flatter than that with the steel reflector (which is peaked in the outer part of the core).] Some attempt was made to account for the different enrichments and number of Gd

 Ricerca Sistema Elettrico	Sigla di identificazione	Rev.	Distrib.	Pag.	di
	PAR2010-ENEA-LD2-010	0	L	6	15

rods between the various configurations, but no firm conclusions were reached as to the reliability of the in-core results produced in this work and the situation is left open.

2.5 Neutron Source Coupling

Concerning the steps taken between writing the fission source in the eigenvalue calculation and reading it in a fixed source calculation, an interface program was written that reads the “mctal” file written by the MCNP eigenvalue calculation and converts it into a form that is readable by the MCNP fixed source calculation. The following points may be mentioned:

- FORTRAN 77 program (1185 lines)
- reads five “mctal” files, one for each assembly type
- expects tallied fission source on mctal file to be in a particular structure
- writes two files (+ standard output):
 - ‘sor4tpe’ (direct access) containing the pin and assembly array elements and the axial segments;
 - ‘sor3tpe’ (unformatted) containing the cumulative probabilities.
- note the standard output contains the axial distribution for the independent source variable “ext” for the ‘sdef’ run.


It may be noted that for the source distribution a pin-by-pin radial description was employed (and thus consistent with the geometry model) and with 21 axial bins (including 8 bins each of height 2 cm to model the spacer grids). The source was read into MCNP from the two files: the unformatted control file and the direct access file for the pin and assembly positions. The following points may be mentioned:

- standard sdef structure in input maintained
- independent variable is “ext”
- dependent variables are: “rad” (in this example it does not actually need to be dependent), “pos” and “cel”.
- only “cel” entries are not physical and are present in given form to intervene in particular places in the code to sample from the ‘sor3tpe’ entries and read the assembly and pin element from ‘sor4tpe’.

MCNP5 was modified to sample and read the radial source position from sor3tpe/sor4tpe and also to sample correctly in the case of rejection (when a pin intersects one of the reflection surfaces and the sampled position is the wrong side of the surface). The latter question has been documented elsewhere. Four subroutines were modified:

- MAIN
- MSGCON (only for message passing)
- MSGTSK (only for message passing)
- SOURCB

Integral core parameters (total power, total neutron source), generated with the fixed fission source read from file, were compared with the estimation of k_{eff} in the eigenvalue calculation (that wrote the fixed source). The small differences observed were due to the spatial discretization of the source (presumably mainly the axial discretization).

 Ricerca Sistema Elettrico	Sigla di identificazione	Rev.	Distrib.	Pag.	di
	PAR2010-ENEA-LD2-010	0	L	7	15


2.6 Ex-Core Transport

The calculation was then made from the core out to the ex-core detectors. For all ex-core calculations, variance reduction with the in-house Direct Statistical Approach was employed (see Appendix).

The heterogeneous nature of the heavy steel reflector was modelled and showed that the homogeneous reflector model was in fact an excellent approximation.

A standard ex-core detector model was employed. The response of interest was the $^{10}\text{B}(n,\alpha)$ rate on an amorphous film on the inner surface of the inner steel cylinder (a thin enough film so that it did not perturb the neutron flux). [The inner steel cylinder was separated from an outer one by a thickness of polyethylene with a thin (1 mm) thickness of cadmium. On the side of the detector facing the core, the cadmium was outside the polyethylene. Instead on the side away from the core, the cadmium was inside the polyethylene.] The detector was placed at two radial positions: in contact with the concrete of the PV well and in contact with the outer surface of the PV. The sensitive part of the detector was assumed to extend axially over 1/2 the physical length.

The results show that the steel reflector reduces the signal in the ex-core detectors from the fundamental mode fission distribution by a factor of between 2 and 3 depending on whether the detector is in contact with the PV or in contact with the concrete.

 Ricerca Sistema Elettrico	Sigla di identificazione	Rev.	Distrib.	Pag.	di
	PAR2010-ENEA-LD2-010	0	L	8	15

3. ²⁵²Cf Start-Up Sources

As far as the primary ²⁵²Cf start-up sources were concerned, the source data were supplied in IRSN DSR/ST3C/XXXX-XX [and following exchange of e-mails (see acknowledgement)]. The nuclear data were the same as those employed in the fundamental fission mode calculation (see §2.1).

3.1 Geometry

For these calculations, a full 360° core model was employed with a pin-by-pin description. The assemblies containing the primary sources were explicitly modelled. The ex-core detectors were assumed in contact with the PV.

3.2 ²⁵²Cf Sources – to – Fundamental Mode


As a first exercise, it was of interest to obtain an indication of how many cycles are required to get from the primary source to the fundamental mode. Shannon entropy was employed to give an indication of this. A plot of the Shannon entropy and the estimate of k_{eff} for the first 100 cycles (each cycle containing 250000 fission neutrons) indicated that more than 200 cycles would be required to reach the fundamental mode. Current calculations indicate that actually between 1000 and 1500 cycles are required. (Note that this concerns a whole core calculation on 360° and not the 1/8 azimuthal segment with reflection surfaces used for the fundamental mode calculations.) This does not in any case affect the results presented here.

3.3 Ex-Core Transport


For the results with the primary source, it should be borne in mind that the energy spectrum of ²⁵²Cf spontaneous fission neutrons is substantially harder than a neutron-induced ²³⁵U fission spectrum.

For the boron concentration that provided 0.95 criticality for the heavy steel reflector model, the ex-core detector responses were generated for 2 of the 3 ex-core detectors and for each of the 6 sources (3 assemblies each with 2 sources), for the homogeneous heavy steel reflector and for the water detector. The fissions were switched off. Considering all 6 sources, the ratio of the signal in the ex-core detectors with water and with steel reflector is substantially higher (between 5 and 6) than the value between 2 and 3 found previously for the fundamental mode. Now the question was what the ratio would be when fissions were included.

The fissions were then switched on (for a maximum of 160 cycles) and the same results were generated as for the case without fissions. Note that at this level of criticality, 160 fission cycles is enough to give the sum over all cycles. The following MCNP5 subroutines were modified to do this: HSTORY, ACECOL. It turns out that even at 0.95 criticality, more than 90% of the signal in the ex-core detectors comes from induced-fission neutrons rather than from the spontaneous fission neutrons of the start-up primary source, this for both the steel and water reflectors (the percentage is higher for the steel reflector compared with the water reflector). As a consequence the above ratio of between 5 and 6 (without fissions) was substantially lowered to between 3 and 4. This also allowed the trend of the ratio over all levels of criticality to be estimated.


 Ricerca Sistema Elettrico	Sigla di identificazione PAR2010-ENEA-LD2-010	Rev. 0	Distrib. L	Pag. 9	di 15
--	---	------------------	----------------------	------------------	-----------------

The differential detector response per fission cycle (up to a maximum of 160 cycles) has also been generated for the cases of the heavy steel reflector and for the water reflector and for the two boron concentrations that provide criticality and 0.95 criticality. Clearly visible are the different effects of the attenuating properties of the steel and water reflectors on the harder spontaneous fission ^{252}Cf spectrum compared with the induced-fission ^{235}U spectrum. (Steel attenuates the more energetic neutrons more than water.) Further modifications were made to subroutines ITALLY and TALLY in MCNP5 to carry this out.

 Ricerca Sistema Elettrico	Sigla di identificazione PAR2010-ENEA-LD2-010	Rev. 0	Distrib. L	Pag. 10	di 15
--	---	------------------	----------------------	-------------------	-----------------


4. Fast Neutron Flux

Finally the fast neutron flux (> 625 keV) in the assemblies directly opposite the ex-core detectors has been calculated for the fundamental mode and for the primary ^{252}Cf source. This information was specifically requested. The flux in the assembly containing the primary ^{252}Cf source (adjacent to the assembly directly opposite the ex-core detectors) is also given.

 Ricerca Sistema Elettrico	Sigla di identificazione PAR2010-ENEA-LD2-010	Rev. 0	Distrib. L	Pag. 11	di 15
--	---	------------------	----------------------	-------------------	-----------------

5. Summary

The effect of the heavy steel reflector (compared with current PWR reflector configurations) on the signal in the ex-core neutron detectors has been estimated for the fundamental fission mode and for the primary ^{252}Cf start-up sources (at 0.95 and at criticality). An estimate of this effect is also made for all criticality levels. As well as being able to compare the signal from different reflector configurations, the normalization of the results (detector counts per second for the ^{252}Cf sources and detector counts per watt of reactor power per second for the fundamental mode) allows the point during reactor start-up when the signal from the fundamental mode becomes predominant compared with the signal from the primary start-up sources, to be estimated.


 Ricerca Sistema Elettrico	Sigla di identificazione PAR2010-ENEA-LD2-010	Rev. 0	Distrib. L	Pag. 12	di 15
--	---	------------------	----------------------	-------------------	-----------------

6. Next Steps

The above represents the situation as at the 1st Nov. 2011. IRSN have requested two further items:

- the change in the primary source (^{252}Cf) results on moving the assemblies containing the primary sources one position towards the core centre.
- results for the secondary (Sb-Be) sources in a form that allows a comparison with the results from the primary sources.


These activities are underway and should be completed by the end of 2011.

 Ricerca Sistema Elettrico	Sigla di identificazione PAR2010-ENEA-LD2-010	Rev. 0	Distrib. L	Pag. 13	di 15
--	---	------------------	----------------------	-------------------	-----------------

Acknowledgements: G. Glinatsis ran NJOY to provide the in-house neutron and n- γ data.

Thanks to B. Normand for supplying and clarifying the geometry and source data.

O. Dubois supplied the AREVA and EdF assembly configurations and power profiles.

 Ricerca Sistema Elettrico	Sigla di identificazione	Rev.	Distrib.	Pag.	di
	PAR2010-ENEA-LD2-010	0	L	14	15

Appendix: the DSA

The Direct Statistical Approach (DSA) was developed in the 1980's and 1990's to optimize Monte Carlo deep penetration (fixed source) radiation transport calculations. It is based on a detailed mathematical approach to the splitting and Russian roulette problem, independent of, or dependent on, the weight of the particle track.

As it relies on splitting and Russian roulette, it is of quite general application and has been employed on a wide variety of applications: reactor shielding, accelerator shielding, Accelerator-Driven Systems, dosimetry and nuclear medicine.

The original development culminated in the general surface parameter model. This was followed by the volume parameter model and the cell importance model. Extensions were made to include contributions to the second moment other than those from track splitting and a weight dependence was introduced. The final development of note was the inclusion of a multi-response capability.

Comparisons have been made of the single response DSA with various versions of the "weight window generator". In general differences tend to appear when large splitting is required, for example when the particle importance varies highly with scattering angle. It should however be emphasized that user experience is key. Also the amount and kind of information on the optimization given back to the user by the variance reduction method is crucial.


Since its incorporation, the multi-response capability has been employed in all the fields listed above. The author's experience is that this feature has totally supplanted the single-response capability in design calculations.

The DSA forms explicit expressions for the second moment S^2 and the time, τ , of a general source particle history as a function of the variance reduction parameters η . The parameters η may be space/energy cell importances or space/energy cell track weights (the DSA "weight line" model condenses the usual weight window to a single value or line).

Monte Carlo is used to generate the coefficients of the second moment and time functions and until recently employed as vehicle a patched version of MCNPX. The parameters η are then found in a separate minimization code that employs a commercial library (IMSL). Usually, as for the weight window generator, a few iterations are made. The coefficients may be accumulated between the iterations but usually instead they are zeroed at the beginning of each iteration.

The version of the DSA that was running until 2010 was unmodified since 2000. Since then, computers have become faster, parallelism has become standard and the range of problems brought within the Monte Carlo scope has greatly increased. As a consequence when applying the DSA to the kind of deep penetration problems that are resolved today with Monte Carlo, some important deterioration (*viz.* slow-down) in performance was noted, especially when using the multi-response capability.

The main bottleneck was in the generation of the coefficients of the second moment function S^2 . (The second moment function employs an approximation called the "enhanced point-surface algorithm". This allows a reasonable approximation to the second moment to be calculated in an acceptable CPU time. The downside is that the amount of data required to define the approximate function is very much larger than the amount required for the exact second moment function.) The coefficients were generated with scalar code based on FORTRAN 77. In the presence of a number of responses (typically up to around 20), energy groups (around 10 neutron and 8 gamma) and 80 or so spatial regions (often unions of MCNP cells), the book-keeping had slowed down the running time considerably. As a result, the time

 Ricerca Sistema Elettrico	Sigla di identificazione	Rev.	Distrib.	Pag.	di
	PAR2010-ENEA-LD2-010	0	L	15	15

employed to generate tracks had become a small (10-20%) fraction of the total computing time, which was unacceptable, especially with the scalar code constraint.

The cause of this slowdown was the employment of a single array within which, by means of pointers, all the variables necessary to characterize the second moment function coefficients were defined. (There were actually a number of hierarchical levels, with pointers pointing into a lower level that itself contained pointers pointing into a lower level, etc.) The lengths of the arrays that the pointers defined were not themselves *a priori* known. As a consequence increasing the bounds of an array at a low level in the hierarchy required considerable data manipulation. This is where the time was lost.

In 2010 a substantial upgrade of the DSA to MCNP5 and MPI was made.

The above-mentioned single array was broken up into its components and the dynamic storage allocation feature of FORTRAN 90 employed on each component array. This speeded-up the generation of the second moment coefficients.

As far as parallelization is concerned, a different situation exists to that of simple Monte Carlo tracking. Instead of requiring the same amount of work at each rendezvous, the DSA requires increasing amounts of work to integrate the second moment arrays generated on each CPU with the current array, as the calculation proceeds. This is because the second moment function expands as the number of particle tracks increases. (Theoretically with the employment of the enhanced point-surface algorithm, the second moment function should saturate once all coefficients are found. Further tracking would then improve the quality of each coefficient. Instead, in practice, this saturation point has never been reached in any realistic calculation. Notwithstanding, the approximate second moment function provides satisfactory “optimized” parameters.)

Parallelization does not therefore supply the same speed-up between scalar and parallel as that obtained with simple Monte Carlo tracking. The speed-up also depends strongly on the number of rendezvous points. In fact the best speed-up is obtained with a single rendezvous for the second moment (and time) function at the end of the calculation. Furthermore after the tracking has finished, all the slaves are put to work simultaneously together with the master to accumulate the second moment (and time) function in the most efficient manner. This is so as to minimize “dead” time at the end of the tracking with the master working while the slaves do not.

Finally, whilst the DSA has continued to employ as vehicle MCNP, the latest patch has been rendered more modular so that it might reasonably easily be attached to another Monte Carlo code.